Available online at www.sciencedirect.com
ScienceDirect
Earth and Planetary Science Letters 261 (2007) 1–8
EPSL
www.elsevier.com/locate/epsl

Hidden Dykes detected on Ultra Long Period seismic signals at Piton de la Fournaise volcano?

Nicolas Houlié [a,*], Jean-Paul Montagner [b]

[a] Berkeley Seismological Laboratory, University of California — 205, Mc Cone Hall — CA 94720-4760 Berkeley, USA
[b] Equipe de Sismologie, Institut de Physique du Globe de Paris, France

Received 17 June 2006; received in revised form 3 April 2007; accepted 5 April 2007
Available online 19 April 2007
Editor: C.P. Jaupart

Abstract

Broadband seismic data enable us to test whether Ultra Long Period (ULP) signals can be used to investigate magma chamber pressure state and to monitor volcanic eruptions. By systematically investigating seismic signals at GEOSCOPE station RER, we find ULP signals associated with volcanic events, during the last 2 decades. We tentatively propose to interpret these signals as events highlighting the activity of the upper magma feeding system of the Piton de la Fournaise volcano and as being related to the deep magma chamber. Some of these unusual signals were previously detected and usually interpreted in term of tilt [Battaglia, J., Aki, K., Montagner, J.-J.-P. Tilt signals derived from a GEOSCOPE VBB station on the Piton de la Fournaise volcano, Geophys. Res. Lett. 27 (5) (2000) 605–608.]. They are detected using STS1 seismometers sensitive in the bandwidth 10^{-3} to 10^{-2} Hz.

This alternative model enables to quantify each event in terms of a pressure drop in the upper magma reservoir of the volcano. Two kinds of seismic waveforms can be associated with two types of fracturing events. The first one is related to the fast rise of a magma batch coming from the deep magma chamber and the second is the result of a slow rise in pressure inside a shallow reservoir. In both cases, we are able to detect these events on very long period seismic data. The interpretation of these signals supports the idea of a single magma source at the sea level. Thus, we propose to classify all the eruptions occurring during the last two decades into two groups, corresponding to the two primary pressure states of the magma chamber.
© 2007 Elsevier B.V. All rights reserved.

Keywords: Ultra Long Period event; Piton de la Fournaise; volcanology; Hidden Dykes

1. Introduction

Both the magma feeding system geometry and the total volume of magma injected in the volcanic edifices still remain poorly known. This constitutes one of the main limitations for a better understanding and prediction of volcanic eruptive events. However, while the existence of a magma chamber is still debated on several volcanoes, it is often observed on paleo-volcanoes around the world (Gudmundsson, 2002). The tracking of magma in motion within the volcanic feeding system is thus a key challenge of modern volcano-seismology.

The Réunion island was created by the Réunion hotspot and is the most recent island of the Mascarene chain. Piton de la Fournaise is one of the two strato-volcanoes located on the eastern part of Réunion Island (France). Following the quiescent period between 1992 and 1998, the volcano has been quasi continuously

* Corresponding author. Tel.: +1 510 642 2601.
E-mail address: houlie@seismo.berkeley.edu (N. Houlié).

0012-821X/$ - see front matter © 2007 Elsevier B.V. All rights reserved.
doi:10.1016/j.epsl.2007.04.018

active since the March 1998 event. The quality of the erupted basalts has been constant during the last two centuries and was described as a “steady state basalt” (Albarède et al., 1997).

The geometry of the magma feeding system is still debated. Some authors suggest that the magma feeding system is complex and composed of small magma reservoirs (Lénat and Bachèlery, 1990) but the large deformations of the whole volcano cannot be explained by such small subsurface sources (Houlié, 2005). It is now generally agreed that there is an upper magma chamber located (we will refer to this magma chamber as P_2 (Aki and Ferrazzini, 2001) at sea level (Nercessian et al., 1996; Sigmundsson et al., 1999; Aki and Ferrazzini, 2001). The volume of the upper magma chamber is estimated to be $5 \cdot 10^8$ m^3 (Sigmarsson et al., 2005). Gravimetry measurements made along an East–West profile across the volcano have been used to locate the upper magma chamber (Lesquer, 1990). Its location is coincident with the observed seismicity (Nercessian et al., 1996; Battaglia et al., 2005). The proposed volume of the magma chamber is large enough (radius ~ 500 m) to deform the whole volcano far away from the summit and west of the Enclos Fouqué, as is observed (Houlié, 2005). On the other hand, while the proposed size for the magma chamber is in agreement with geochemical measurements, it would be undetectable to seismic imaging. The migration of fluid coming out of this upper magma chamber and circulating inside the edifice can be detected by deformation at the surface.

The use of long period (LP) or very long period (VLP) seismic events (0.2 Hz ≤ f ≤ 0.5 Hz) has been successfully applied to several volcanoes (Chouet, 1988, 1992; Chouet et al., 1994; Neuberg et al., 1994; Falsaperla et al., 1994; Uhira and Takeo, 1994; Chouet, 1996a,b; Kaneshima, 1996; Gil Cruz and Chouet, 1997; Okubo et al., 1997; Wassermann, 1997; Ohminato et al., 1998; Rowe et al., 1998; Arciniega-Ceballos et al., 1999; Chouet et al., 1999; Hidayat et al., 2000; Kumagai et al., 2000; Legrand et al., 2000; Kawakatsu, 2000; Aster et al., 2000; Stephens and Chouet, 2001; Hill et al., 2002; Hidayat et al., 2002; Kumagai et al., 2002a, b; Almendros et al., 2002; Arciniega-Ceballos et al., 2003; Nakano et al., 2003; Chouet et al., 2003; Chouet, 2003; Dawson et al., 2004; Chouet et al., 2005; Zobin et al., 2005; McNutt, 2005; Kumagai et al., 2005; Auger et al., 2006; Kumagai, 2006; Kumagai and Chouet, 1999) in order to investigate fluid circulation inside several volcano edifices.

We present seismological evidences for a long-term response of the volcano to the deformation induced by changes in pressure inside the magma chamber located at sea level. The seismic signals are associated with the main eruptive events and recorded in the 10^{-3}–10^{-2} Hz frequency range.

2. Data

In this study, we use data recorded by the permanent broadband seismometer (3 components Streckeisen STS1 (Wielandt and Streckeisen, 1982) located in the valley formed by the *Riviere de l'Est* on the northern flank of the volcano (21.159 S, 55.746 E, 834 m a.s.l.). This station belongs to the GEOSCOPE (Romanowicz et al., 1984; Montagner et al., 1998; Roult et al., 2005) global seismic network under the code name RER (Fig. 1).

The RER station is located 8 km north of the volcano summit and 800 m above sea level (Fig. 1). The location of the instrument allows it to experience millimetric (and even micrometric) displacement due to magma chamber deformation. Due to a vertical accuracy estimated at ±15 mm, permanent GPS receivers located at the summit (Fig. 2) and above the magma chamber are not sensitive enough to measure millimetric deformation. The seismometer records instantaneous velocity on three different acquisition channels, BH, LH and VH, which record ground motions with sampling rate of 0.05, 1 and 10 s respectively. We investigated the LH channel having removed the response in displacement using SAC software (Goldstein et al., 2000). We

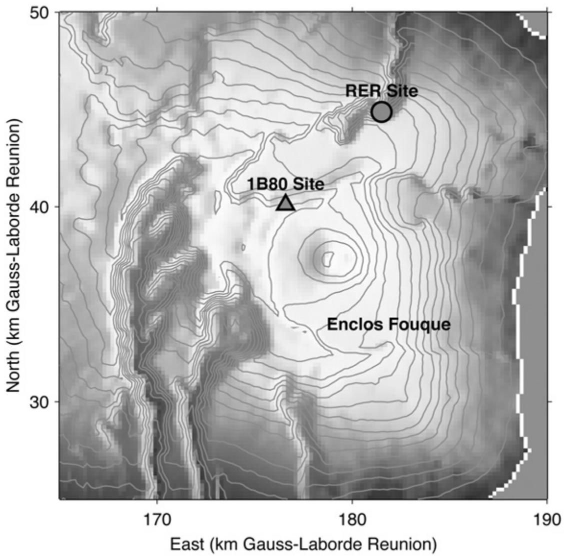

Fig. 1. Topography of the Piton de la Fournaise. The GEOSCOPE site (RER) is denoted by the gray circle and located in the Riviere de l’Est. The GPS 1B80 site is denoted by the gray triangle. The scale is indicated in km (Gauss–Laborde Reunion reference Frame).

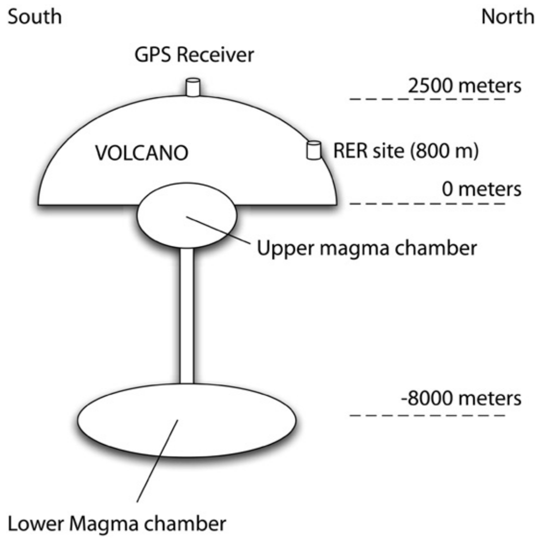

Fig. 2. North–south cross-section of the volcano.

systematically analyzed all the data available at the volcanic event dates in the GEOSCOPE dataset for RER between 1992 and 2006. The continuous waveforms for the main eruptive events are presented in Fig. 3 and in additional material (Fig. A1, A2, A3).

On each seismogram, we see a step in velocity particularly on the north–south (N–S) component. This step is then followed by a slow recovery of the velocity during the following couple of hours. The East–West component is also affected but the observed amplitudes are always smaller. The vertical component does not show a correlated signal. This suggests that the N–S signal represents the radial deformation and that the altitude of the source and the altitude of the RER site are similar. While many glitches or spikes are visible on the velocity records, they are no longer visible on displacement records. Therefore, the steps visible on the North–South component cannot be due to misfunctioning of the seismometer. They have been previously observed (Battaglia et al., 2000) and interpreted in term of tilt. However, two different kinds of signal can be observed according to the eruptions. The first kind corresponds to a positive impulse followed by a negative step which slowly decreases with time and the second type of signal is a negative transient also slowly decreasing.

3. Results

The radius of the upper magma chamber located at the sea level is estimated to be 500 m (Sigmarsson et al., 2005). The shear modulus μ of the Piton de la Fournaise is estimated to be ~2 GPa in agreement with an overpressure (50 MPa) of the whole magma system (Rubin and Pollard, 1987) and with observation of GPS time-series of the 1B80 GPS benchmark (Fig. 1) located outside the Enclos Fouqué (Houlié, 2005). This value is also close to previous estimates of μ made on other volcanoes (Rubin and Pollard, 1987; Mériaux and Jaupart, 1995; Cayol and Cornet, 1998).

As we are observing signals at a single site, we have chosen to explain the data assuming the tilt contribution (Wielandt and Forbriger, 1999; Battaglia et al., 2000) is low with respect to a possible contribution of displacement.

At the RER site, after correcting the data (Fig. 3) for the instrument response, it is possible to assess the pressure drop ΔP in the magma chamber by using the following equation describing the displacement Δd associated with a deflating/inflating point source (Mogi, 1958):

$$\Delta P = \frac{4\mu\Delta d}{3a^3}\frac{(D^2+F^2)^{\frac{3}{2}}}{D} \quad (1)$$

where D and F are the horizontal and vertical distances respectively between the point source and RER, a the radius of the magma chamber, μ the shear modulus and Δd the associated horizontal displacement measured at RER. Following this equation the horizontal displacement Δd is equal to zero above the source ($D=0$). In this area, the horizontal and vertical distances D and F are equal to 800 and 8000 m respectively. The estimated changes of pressure are in good agreement with the lithostatic pressure above the magma chamber (~70 MPa). This suggests that we observe a transfer of mass subsequent to magma-chamber rupture as a result of overpressure action. The activity reports of the IPGP observatory (Staudacher and P. de la Fournaise research Team, 1992–2006) allow us to estimate the rising velocity of the magma (from 0.03 to 1.39 m per second, (Table 1) from the summit of the magma chamber to the surface.

We can estimate the change of volume inside the magma chamber during the event using the following relationship (Tait et al., 1989):

$$\Delta V = \frac{3V}{4\mu}\Delta P \quad (2)$$

ΔV is an upper bound since we neglect tilt.

The computed volumes of extruded magma are not linearly related to the seismic swarm durations except for the 2000's events. There is a linear relationship for small eruptive events in 2000 ($\Delta V \leq 10^6$ m^3) between the time–duration of the seismic crisis (Peltier et al., 2005) and the volume of magma extruded from the

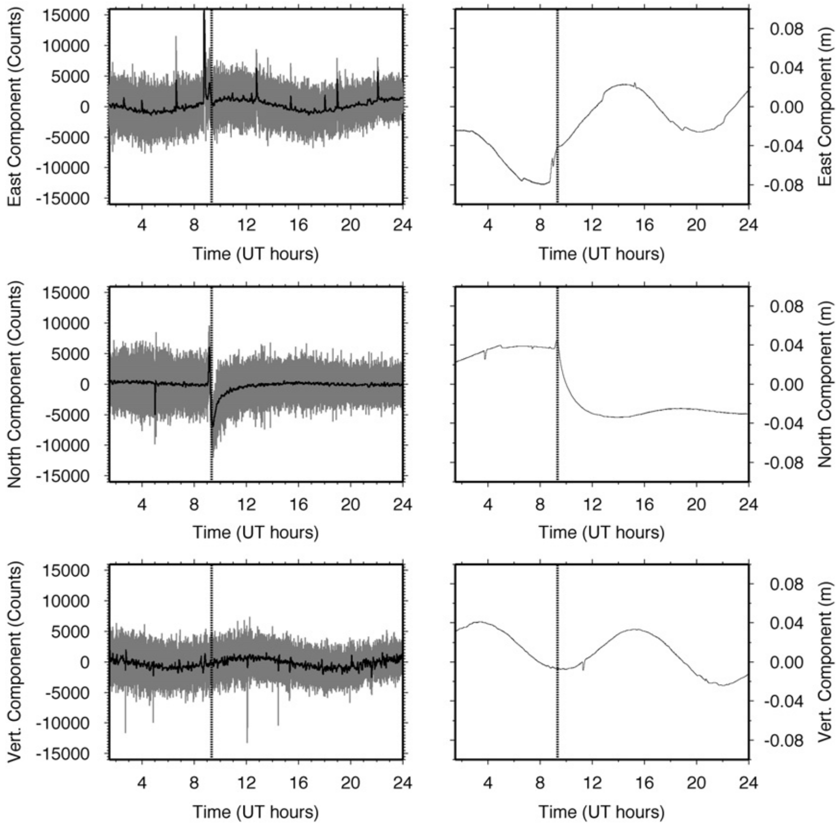

Fig. 3. March 27th 2001. Left: GEOSCOPE data, in counts (the data are filtered by using a lowpass filter of 10^{-2} Hz). The three components of the LH channel (the sampling rate is equal to 1 s) are plotted. A deformation is detected by the broadband seismometer on the two horizontal components of the seismogram. Right: After applying the response of the instrument, the associated displacement on the Northern component is equal to ~65 mm. Right Column is displacement (in meter). The time of the eruptive event is indicated by a grey vertical line.

magma chamber. This relationship is not valid for larger eruptions. This suggests that the magma feeding system remains open a long time after the start of the eruption and the magma chamber is initially broken (Gudmundsson, 2006). For a smaller eruptive event, the dyke extending from the magma chamber should be sealed after a short time. As no additional deflation is observed after the pressure step associated with a velocity change, we suggest that new batches of magma are continuously coming from the deeper magma chamber, going through the upper magma chamber and reaching the surface of the volcano.

The extruded volume during the March 1998 event remains uncertain and is based only on the north–south component observations (~−9000 counts). In this case, the instrumental responses were not applied because glitches are present on data. We have used the March 2001 signal to estimate the March 1998 volume (the instrument responses are the same). The volume modelled to explain the deformation of the volcano in March 1998 is at least to 2 million m^3 but inferior to 4 million m^3 (Battaglia and Bachèlery, 2003; Sigmundsson et al., 1999). This volume is small compared to the total erupted volume (510^7 m^3) which is of the same order of magnitude as the volume estimated by our method (Table 1). This result suggests a volume, equal to half of the total volume erupted at the surface in the March 1998 event, was injected in less than 2 h in the volcano without reaching the surface.

If our interpretation of data is correct, two main types of events are related to the general activity of the volcano. Since we observe two kinds of seismic waveforms, they might correspond to two types of events. We estimated an alternative explanation of the signals can be put forward in terms of displacement instead of tilt as previously proposed (Battaglia et al., 2000; Battaglia and Bachèlery, 2003). The first type of volcanic event is related to the arrival of a new batch of magma (23 August 1992, 28 September 1999, 23 June 2000, 27 March 2001 and 11 June 2001) while the other events (8 March 1998, 11 October 2000, 15 November 2002, 17 February 2005, 29 November

Table 1
Over-pressure and volume estimates

Date	Eruption date	Δd (mm)	ΔP (MPa)	ΔV (10^6 m^3)	Travel time	Estimated velocity (m/s)	Type
1992, Aug. 27, 0703	1992, Aug., 27, 0750	35±5	−48.5±3.5	−9.5±0.4	0 h 47 min	0.60–0.89	1
1998, Mar. 8, 0949	1998, Mar. 9, 1105			~20 [a]	2 h 16 min	0.21–0.31	2
1999, Jul. 19, 1134	1999, Jul., 19, N/A	50±2	−69.3±1.4	−13.6±0.1			1
1999, Sep. 28, 0713	1999, Sep., 28, 0758	22±2	−30.5±1.4	−6.0±0.1	0 h 45 min	0.63–0.93	2
2000, Feb. 14, 1933	2000, Feb., 14, N/A	30±10	−41.6±7.0	−8.1±0.3			1
2000, Jun. 23, 1303	2000, Jun. 23, N/A	40±3	−55.4±2.1	−10.9±0.2			2
2000, Oct. 11, 1119	2000, Oct. 12, 0105	60±5	−83.2±3.5	−16.3±0.4	13 h 46 min	0.03–0.05	2
2001, Mar. 27, 0843	2001, Mar. 27, 0920	65±15	−90.1±1.0	−17.6±1.0	37 min	0.77–1.13	1
2001, Jun. 11, 0920	2001, Jun. 11, 0950	50±4	−69.3±3.0	−13.6±0.3	0 h 30 min	0.94–1.39	1
2002, Nov., 15, 2003	2002, Nov. 16, 0033	50±2	−69.3±1.4	−13.6±0.1	4 h 30 min	0.010–0.15	2
2005, Feb. 17, 1343	2005, Feb., 17, 1635	40±5	−55.4±3.0	−10.9±0.3	2 h 52 min	0.16–0.24	2
2005, Nov. 29, 0151	2005, Nov. 29, 0225	20±2	−27.7±1.4	−5.4±0.1	34 min	0.83–1.23	2
2005, Dec. 26, 1048	2005, Dec. 26, 1315	60±5	−83.2±3.0	−16.3±0.3	2 h 27 min	0.19–0.28	2

All volumes are estimated from the displacement on the north–south component after removing the instrumental response in displacement on the LH (1 Hz) or BH (20 Hz) channel. The volume of the magma chamber is equal to ~500 mm^3. The lithostatic pressure above the magma chamber is ~70 · 10^6 m^3. Since the tilt is neglected ΔV constitutes an upper bound of the real volume. The time of the eruptive event are given by OVPF/IPGP (Staudacher and P. de la Fournaise research Team, 1992).

[a] The volume of the 1998 injection is approximate.

2005, 26 December 2005) are related to long-term loading of the shallow magma chamber which are not visible with seismometers but with GPS. During the rapid arrival of a new batch of magma in the upper reservoir, a rapid velocity change is visible on waveforms. Besides, the other type of events are suggesting the magma chamber is in equilibrium with the lower magma system of the volcano (P_1 following Aki and Ferrazzini, 2001).

There is apparently no relationship between the volume erupted and this new classification. A new batch of magma coming into the upper chamber may cause an eruptive event, but not in every instance. It may be possible to determine a pressure threshold for the magma chamber when an eruption would occur, however this threshold might not be constant with time. Furthermore, determining the threshold pressure requires to take into account the mechanical layering, the geometry of the magma chamber, and the loading of the magma chamber.

We have listed in Table 1 the overpressure and changes of volumes computed from the RER seismic data for all volcanic events recorded.

4. Discussion

The estimation of volume change ΔV and its location using a broadband seismometer data is still approximate in the case of the Piton de la Fournaise and the volumes estimated here are constituting an upper bound limit. We are aware that this approach is simplistic but we believe that it is justified by the fact that the Mogi's model is still routinely used in volcano observatories to determine the pressure change in the edifice. A large number of deformation models are available in the literature (Yang and Davis, 1986; Gudmundsson, 1987). Some additional experiments will be necessary to discriminate the relative contributions of tilt and displacement during the transfer of magma out of the upper reservoir. The transient deformations extend over a region larger than 10 km across and with a typical duration of 500–1000 s. The similar pattern of deformation observed suggests that the source of the events has been stable over the last 15 yr. Large scale deformations were already suggested based on GPS benchmark time-series located on the western part of the Enclos Fouqué. We also confirm here that the East–West displacement of the GPS benchmark 1B80 (Fig. 1) could be related to the magma chamber pressure state and not to the slip along a discontinuity located along the border of the Enclos Fouqué, as previously suggested (Houlié, 2005).

The GPS station located at the summit of the edifice constitutes a complementary tool to detect the long-term deformation episodes (T ~ 6 months).

The GPS receivers at the summit are only sensitive to the long-term component of the deformation of the magma chamber (Fig. 4). Due to their location above the source, their sensitivity is reduced to the vertical component accuracy of the GPS (±15 mm) (Houlié, 2005).

The variability of the signal on the eastern component of RER suggests that it might be possible to locate the source of the over/under pressure provided that an additional broadband seismometer survey

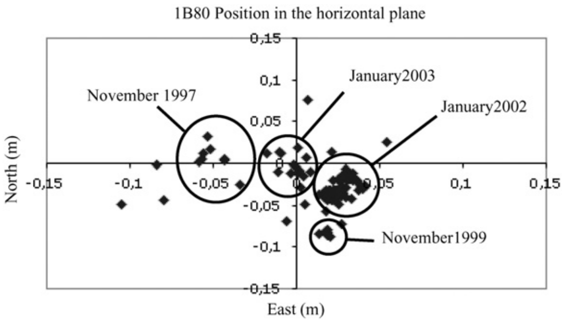

Fig. 4. Displacement of the site 1B80 during 1997–2002 period. The shear modulus μ is estimated to be 1.95 GPa at the Piton de la Fournaise. This low value is similar to the one used in Hawaii (Rubin and Pollard, 1987) to model the injection of basalt at Kilauea volcano. Figure from Houlié (2005). Data: OVPF/IPGP.

network is installed on this volcano. Given the relative amplitudes of the offset on the N–S and E–W components of RER, the source detected here is likely located north-west of the summit which is consistent with the magma chamber location as suggested by gravimetric data (Lesquer, 1990) and previous GPS observations (Houlié, 2005).

This study suggests that large volumes of magma are being injected inside the volcano. Most of this magma is not reaching the surface as observed on paleovolcanic (Gudmundsson, 1995, 2002; Gudmundsson et al., 2005) and during contemporary volcanic events (Houlié et al., 2006).

The GPS network is able to detect the gradual filling of the upper magma chamber (Fig. 4). The associated loads deform the western outer part of the Enclos. As the seismological network is not able to detect the slow deformations ($T \geq 1$ month), the seismic and GPS data are complementary.

The general deformation of the volcano seems to consist of at least three components:

1– A long-term (10 yr) extension equal to 3 mm per year between the IPGP observatory (15 km west of the summit) and the east coast of the island (Houlié, 2005);
2– Deformation related to the injection of magma in provenance of the upper magma chamber ($T \sim 500$ s). These deformations cannot be detected by using strong-motion seismometers;
3– Deformation resulting from the rise of the dyke up to the surface ($1\ \text{s} \leq T \leq 50$ s) detectable by strong-motion seismometers and geodetic networks.

The technique developed in this paper may provide an alternative approach to the prediction of volcanic eruptions, which has so far been based on the study of seismicity activity (Voight, 1988; Collombet et al., 2003; Kilburn and Sammonds, 2005).

Acknowledgements

We are grateful to the GEOSCOPE group and the station managers for providing us with the data. We thank the Observatoire Volcanologique du Piton de la Fournaise (OVPF) for maintaining the Piton de la Fournaise monitoring networks. Authors thank Barbara Romanowicz, Bernard Chouet and Richard Allen for their comments. We thank Thomas Staudacher, Valerie Ferrazzini and Jean Battaglia who pointed some timing errors and provided fruitful critics and suggestions. This is a University of California—Berkeley Seismological Lab. contribution (number 07-03).

Appendix A. Supplementary data

Supplementary data associated with this article can be found, in the online version, at doi:10.1016/j.epsl.2007.04.018.

References

Aki, K., Ferrazzini, V., 2001. Comparison of Mount Etna, Kilauea, and Piton de la Fournaise by a quantitative modeling of their eruption histories. J. Geophys. Res. 106 (B3), 4091–4102.

Albarède, F., Luais, B., Fitton, G., Semet, M., Kaminski, E., Upton, B.G.J., Bachelery, P., Cheminée, J.L., 1997. The geochemical regimes of Piton de la Fournaise volcano (Réunion) during the last 530,000 years. J. Petrol. 38, 171–201.

Almendros, J., Chouet, C., Dawson, P., Bond, T., 2002. Identifying elements of the plumbing system beneath Kilauea Volcano, Hawaii, from the source locations of very-long-period signals. Geophys. J. Int. 148, 303–312.

Arciniega-Ceballos, A., Chouet, B.A., Dawson, P., 1999. Very-long-period signals associated with Vulcanian explosions at Popocatepetl Volcano, Mexico. Geophys. Res. Lett. 26 (19), 3013–3016.

Arciniega-Ceballos, A., Chouet, B.A., Dawson, P., 2003. Long-period events and tremor at Popocatepetl Volcano (1994–2000) and their broadband characteristics. Bull. Volcanol. 65, 124–135.

Aster, R., Lees, J., Neuberg, J., 2000. Seismic and acoustic observations of volcanic seismicity (editorial). J. Volcanol. Geotherm. Res. 101, vii–viii.

Auger, E., D'Auria, L., Martini, M., Chouet, B., Dawson, P., 2006. Real-time monitoring and massive inversion of source parameters of very long period seismic signals: an application to Stromboli Volcano, Italy. Geophys. Res. Lett. 33 (L04301), 1–5.

Battaglia, J., Bachèlery, P., 2003. Dynamic dyke propagation deduced from tilt variations preceeding the March 9, 1998, eruption of the Piton de la Four-naise volcano. J. Volcanol. Geotherm. Res. 120, 289–310.

Battaglia, J., Aki, K., Montagner, J.-J.-P., 2000. Tilt signals derived from a GEOSCOPE VBB station on the Piton de la Fournaise volcano. Geophys. Res. Lett. 27 (5), 605–608.

Battaglia, J., Ferrazzini, V., Staudacher, T., Aki, K., Cheminée, J.-L., 2005. Pre-eruptive migration of earthquakes at the Piton de la Fournaise volcano (Réunion Island). Geophys. J. Int. 161, 549–558.

Cayol, V., Cornet, F.H., 1998. Effects of topography on the interpretation of the deformation field of prominent volcanoes; application to Etna. Geophys. Res. Lett. 25, 1979–1982.

Chouet, B., 1988. Resonance of a fluid-driven crack: radiation properties and implications for the source of long-period events and harmonic tremor. J. Geophys. Res. 93, 4375–4400.

Chouet, B., 1992. A seismic model for the source of long-period events and harmonic tremor. In: Gasparini, P., Scarpa, R., Aki, K. (Eds.), Volcanic Seismology. Springer-Verlag, Berlin, pp. 133–156.

Chouet, B., 1996a. Long-period volcano seismicity: its source and use in eruption forecasting. Nature 380, 309–316.

Chouet, B., 1996b. New methodology and future trends in seismological monitoring. In: Scarpa, R., Tilling, R. (Eds.), Monitoring and Mitigation of Volcano Hazards. Springer-Verlag, pp. 23–97.

Chouet, B., 2003. Volcano seismology. Pure Appl. Geophys. 160, 739–788.

Chouet, B.A., Page, R.A., Stephens, C.D., Laher, J.C., Power, J., 1994. Precursory swarms of long-period events at Redoubt Volcano (1989–1990), Alaska; their origin and use as a forecasting tool. J. Volcanol. Geotherm. Res. 62, 95–135.

Chouet, B., Saccorotti, G., Dawson, P., Martini, M., Scarpa, R., DeLuca, G., Milana, G., Cattaneo, M., 1999. Broadband measurements of the sources of explosions at Stromboli Volcano, Italy. Geophys. Res. Lett. 26, 1937–1940.

Chouet, B., Dawson, P., Ohminato, T., Martini, M., Saccorotti, G., Giudicepietro, F., De Luca, G., Milana, G., Scarpa, R., 2003. Source mechanisms of explosion at Stromboli Volcano, Italy, determined from moment-tensor inversions of very-long-period data. J. Geophys. Res. 108 (B1), 2019.

Chouet, B., Dawson, P., Arciniega-Ceballos, A., 2005. Source mechanism of Vulcanian degassing at Popocatépetl Volcano, Mexico, determined from waveform inversions of very long period signals. J. Geophys. Res. 110 (B07301), 1–20.

Collombet, M., Grasso, J.-R., Ferrazzini, V., 2003. Seismicity rate before eruptions on piton de la fournaise volcano: implications for eruption dynamics. Geophys. Res. Lett. 30 (21), 2099.

Dawson, P., Whilldin, D., Chouet, B., 2004. Application of near real-time radial semblance to locate the shallow magmatic conduit at Kilauea Volcano, Hawaii. Geophys. Res. Lett. 31 (L21606), 1–4.

Falsaperla, S., Langer, H., Martinelli, B., Schick, R., 1994. Seismic measurements on Stromboli Volcano in a wide frequency range. Acta Vulcanol. 5, 173–178.

Gil Cruz, F., Chouet, B.A., 1997. Long-period events, the most characteristic seismicity accompanying the emplacement and extrusion of a lava dome in Galeras Volcano, Colombia, in 1991. J. Volcanol. Geotherm. Res. 77, 121–158.

Goldstein, P., Dodge, M., Firpo, M., Minner, L., 2003. SAC2000: Signal Processing and Analysis Tools for Seismologists and Engineers. The IASPEI International Handbook of Earthquake and Engineering Seismology.

Gudmundsson, A., 1987. Formation and mechanics of magma reservoirs in Iceland. Geophys. J. R. Astron. Soc. 91, 27–41.

Gudmundsson, A., 1995. Infrastructure and mechanics of volcanic systems in Iceland. J. Volcanol. Geotherm. Res. 64, 1–22.

Gudmundsson, A., 2002. Emplacement and arrest of sheets and dykes in central volcanoes. J. Volcanol. Geotherm. Res. 116, 279–298.

Gudmundsson, A., Ingrid, I., Loetveit, F., 2005. Dyke emplacement in a layered and faulted rift zone. J. Volcanol. Geotherm. Res. 144, 311–328 (Corrected Proof).

Gudmundsson, A., 2006. How local stresses control magma-chamber ruptures, dyke injections, and eruptions in composite volcanoes. Earth-sci. Rev. 79 (1–2), 1–31. doi:10.1016/j.earscirev.2006.06.006.

Hidayat, D., Voight, B., Langston, C., Ratdomopurbo, A., Ebeling, C., 2000. Broadband seismic experiment at Merapi Volcano, Java, Indonesia: very-long period pulses embedded in multiphase earthquakes. J. Volcanol. Geotherm. Res. 100, 215–231.

Hidayat, D.B., Chouet, B.A., Voight, B., Dawson, P., Ratdomopurbo, A., 2002. Source mechanism of very-long-period signals accompanying dome growth activity at Merapi Volcano, Indonesia. Geophys. Res. Lett. 29 (23), 2118.

Hill, D., Dawson, P., Johnson, M., Pitt, A., Biasi, G., Smith, K., 2002. Very-long period volcanic earthquakes beneath Mammoth Mountain California. Geophys. Res. Lett. 29 (10), 1370.

Houlié, N. Mesure et Modélisation de données GPS de volcans. Applications à des études de déformation à diverses échelles et a` la tomographie des panaches atmosphériques., PhD Thesis, Institut de Physique du Globe de Paris (2005).

Houlié, N., Komorowski, J.-C., de Michele, M., Kasereka, M., Ciraba, H., 2006. Early detection of eruptive dykes revealed by Normalized Difference Vegetation Index (NDVI) on high-resolution satellite imagery. Earth Planet. Sci. Lett. 246 (3–4), 231–240. doi:10.1016/j.epsl.2006.03.039.

Kaneshima, S., 1996. Mechanism of phreatic eruptions at Aso Volcano inferred from near-field broadband seismic observations. Science 273, 642–645.

Kawakatsu, H., 2000. Aso94: Aso seismic observation with broadband instruments. J. Volcanol. Geotherm. Res. 101, 129–154.

Kilburn, C.R.J., Sammonds, P., 2005. Maximum warning times for imminent volcanic eruptions. Geophys. Res. Lett. 32, L24313.

Kumagai, H., 2006. Temporal evolution of a magmatic dike system inferred from the complex frequencies of very long period seismic signals. J. Geophys. Res. 111 (B06201), 1–13.

Kumagai, H., Chouet, B.A., 1999. The complex frequencies of long-period seismic events as probes of fluid composition beneath volcanoes. Geophys. J. Int. 138, L24313 (F7–F12).

Kumagai, H., Ohminato, T., Nakano, M., Ooi, M., Kubo, A., Inove, H., 2000. Very-long-period seismic signals and caldera formation at Miyake Island, Japan. Science 293, 687–690.

Kumagai, H., Chouet, B.A., Nakano, M., 2002a. Temporal evolution of a hydrothermal system in Kusatsu-Shirane Volcano, Japan, inferred from the complex frequencies of long-period events. J. Geophys. Res. 107 (B10), 2236.

Kumagai, H., Chouet, B.A., Nakano, M., 2002b. Waveform inversion of oscillatory signatures in long-period events beneath volcanoes. J. Geophys. Res. 107 (B11), 2301.

Kumagai, H., Chouet, B., Dawson, P., 2005. Source process of a long-period event at Kilauea Volcano, Hawaii. Geophys. J. Int. 161, 243–254.

Legrand, D., Kaneshima, S., Kawakatsu, H., 2000. Moment tensor analysis of near-field broadband waveforms observed at Aso volcano, Japan. J. Volcanol. Geotherm. Res. 155–169.

Lénat, J.-.F., Bachèlery, P., 1990. Structure and dynamics of the central zone of Piton de la Fournaise volcano. Le volcanisme de la Réunion — Monographie, pp. 257–296.

Lesquer, A., 1990. Structure profonde de l'ýˆle de la Réunion d'après les anomalies gravimétriques. In: Lénat, J.F. (Ed.), Le volcanisme de le Réunion. Monographie. CRV, Clermont Ferrand, France, pp. 257–296.

McNutt, S., 2005. Volcano seismology. Annu. Rev. Earth Planet. Sci. 32 (15), 1–31.

Mériaux, C., Jaupart, C., 1995. Simple fluid dynamic models of volcanic rift zones. Earth Planet. Sci. Lett. 136, 223–240.

Mogi, K., 1958. Relations between the eruption of various volcanoes and the deformations of the ground surfaces around them. Bull. Earthq. Res. Inst. Univ. Tokyo 36, 99–134.

Montagner, J.-P., Lognonné, P., Beauduin, R., Roult, G., Karczewski, J.-F., Stutzmann, E., 1998. Towards multiscalar and multiparameter networks for the next century: the French efforts. Phys. Earth Planet. Inter. 108, 155–174.

Nakano, M., Kumagai, H., Chouet, B., 2003. Source mechanism of long-period events at Kusatsu-Shirane Volcano, Japan, inferred from waveform inversions of the effective excitation functions. J. Volcanol. Geotherm. Res. 122, 149–164.

Nercessian, A., Hirn, A., Lepine, J.C., Sapin, M., 1996. Internal structure of piton de la fournaise volcano from seismic wave propagation and earthquake distribution. J. Volcanol. Geotherm. Res. 70, 123–143.

Neuberg, J., Luckett, M., Ripepe, R., Braun, T., 1994. Highlights from a seismic broadband array on Stromboli Volcano. Geophys. Res. Lett. 21, 749–752.

Ohminato, T., Chouet, B.A., Dawson, P., Kedar, S., 1998. Waveform inversion of very long period impulsive signals associated with magmatic injection beneath Kilauea Volcano, Hawaii,. J. Geophys. Res. 103 (12), 23839–23862.

Okubo, P.G., Benz, H.M., Chouet, B.A., 1997. Imaging the crustal magma sources beneath Mauna Loa and Kilauea volcanoes, Hawaii. Geology 25 (10), 867–870.

Peltier, A., Ferrazzini, V., Staudacher, T., Bachèlery, P., 2005. Imaging the dynamics of dyke propagation prior to the 2000–2003 flank eruptions at Piton de La Fournaise, Reunion Island. Geophys. Res. Lett. 32, L22302.

Romanowicz, B., Cara, M., Fels, J., Rouland, D., 1984. GEOSCOPE: a French initiative in long period, three component, global seismic networks. Eos, Trans. - Am. Geophys. Union 65, 753–754.

Roult, G., Lépine, J., Bonaimé, S., Riveira, L., 2005. The GEOSCOPE program: state of the art in 2005. AGU 2005 Fall Meet. Suppl., vol. 86.

Rowe, C., Aster, R., Kyle, P., Schlue, J.W., Dibble, R., 1998. Broadband recordings of Strombolian explosions and associated very-long-preiod seismic signals on Mount Erebus Volcano, Ross Island, Antarctica. Geophys. Res. Lett. 25, 2297–2300.

Rubin, A., Pollard, D., 1987. Origins of blade-like dikes in volcanic rift zone. In: Decker, R.W., Wright, T.L., Stauffer, P. (Eds.), Volcanism in Hawaii. . USGS professional paper, vol. 1350. U.S. Geological Survey, Denver, Colorado, pp. 1449–1470.

Sigmarsson, O., Condomines, M., Bachélery, P., 2005. Magma residence time beneath the Piton de la Fournaise Volcano, Reunion Island, from U-series disequilibria. Earth Planet. Sci. Lett. 234 (1–2), 223–234.

Sigmundsson, F., Durand, P., Massonnet, D., 1999. Opening of an eruptive fissure and seaward displacement at piton de la fournaise volcano measured by radarsat satellite radar interferometry. Geophys. Res. Lett. 26, 533–536.

Staudacher, T., P. de la Fournaise research Team, 1992–2006. Bulletin of the Global Volcanism Network. Smithsonian Institution.

Stephens, C.D., Chouet, B.A., 2001. Evolution of the December 14, 1989 precursory long-period event swarm ar Redoubt Volcano, Alaska. J. Volcanol. Geotherm. Res. 109, 133–148.

Tait, S., Jaupart, C., Vergniolle, S., 1989. Pressure, gas content and eruption periodicity of a shallow, crystallising magma chamber. Earth Planet. Sci. Lett. 92, 107–123.

Uhira, K., Takeo, M., 1994. The source of explosive eruptions of Sakurajima Volcano. J. Geophys. Res. 99, 17775–17789.

Voight, B., 1988. A method for prediction of volcanic eruption. Nature 332, 125–130.

Wassermann, J., 1997. Locating the sources of volcanic explosions and volcanic tremors at Stromboli Volcano (Italy). Phys. Earth Planet. Inter. 104, 271–281.

Wielandt, E., Forbriger, T., 1999. Near-field seismic displacement and tilt associated with the explosive activity of stromboli. Ann Geofis 42 (3), 407–416.

Wielandt, E., Streckeisen, G., 1982. The leaf-spring seismometer; design and performance. Bull. Seismol. Soc. Am. 72 (A), 2349–2367.

Yang, X., Davis, P.M., 1986. Deformation due to a rectangular elastic tension crack in an elastic half-space. Bull. Seismol. Soc. Am. 76, 865–881.

Zobin, M.V., Nishimura, Y., Miyamura, J., 2005. The nature of volcanic earthquake swarm preceding the 2000 flank eruption at Usu volcano, Hokkaido, Japan. Geophys. J. Int. 163, 265–275.